Towards High-Capacity HTS Flywheel Systems

Frank N. Werfel, Uta Floegel-Delor, Thomas Riedel, Rolf Rothfeld, Dieter Wippich, Bernd Goebel, Gerhard Reiner, and Niels Wehlau

***Abstract*—Adelwitz Technologiezentrum (ATZ) and L-3 Communications Magnet Motor (L-3 MM) are currently mounting a compact-designed flywheel energy storage system (FESS) with total magnetic bearing support. Final assembly and test operation were performed during 2008–2009. After calculations and experiments, we decided to improve rotor stabilization by stiffer geometry. In addition, two dynamical emergency bearings contribute to robust and safe flywheel operation in critical revolution-per-minute situations. A planned energy capacity of 5 kWh is now obtained at about 8000 r/min, whereas an increased capacity of 10 kWh will be stored at a speed of 10 000 r/min. The total weight of the flywheel unit is about 1200 kg plus power electronics and cooling system. The heavier 600-kg rotor causes new design and construction work in mechanical elements, magnetic support bearings, cooling, and power electronics. Due to the here reported construction changes and increased rotor speed, scaling to even larger energy storage performance of 15–20 kWh seems achievable. ATZ and L-3 MM obtained a corresponding order to develop and deliver a 15-kWh/400-kW high-temperature-superconducting FESS for a Korean local grid UPS application.**

***Index Terms*—Energy storage, flywheel, rotor dynamics.**

I. Introduction

ADELWITZ Technologiezentrum (ATZ) and L-3 Communications Magnet Motor (L-3 MM) have fabricated a 5-kWh 250-kW flywheel energy storage system (FESS) using two magnetic bearings supporting the 0.6-t rotor. To date, no high-temperature superconducting (HTS) flywheel in continuous operation is available. Several projects are performed in research and development status with total development costs of about some tens of millions U.S.$ [1]–[5]. Most problems of development are associated with rotor dynamics and rotor stabilization by HTS magnetic bearings. Concluding the attempts and reports, it seems that magnetically supported flywheels are definitely not for those with short attention spans. It requires a multidisciplinary team, having expertise in not only superconductivity but material science, magnetics, power electronics, vacuum techniques, and rotor dynamics. Our general flywheel concept and design follow conventional flywheels developed and applied to mobile applications by L-3 MM. When the rotor is suspended by mechanical bearings, a permanent magnet (PM) iron configuration can reduce the axial load, and energy savings of 30%–40% could be obtained in the total energy balance. However, in long-term storage, the total loss per day is 60% or more of the stored energy. Therefore, some groups started in the past the incorporation of HTS magnetic bearings to make FESS concepts beneficial. From the developments and experiments, the enormous complexity of a magnetically stabilized flywheel becomes evident. Rotor dynamics requires high load bearing performance and high stiffness and damping capabilities to operate the flywheel in all situations of charging and discharging. The present HTS flywheel project started in 2005. We developed and analyzed the radial HTS bearing with axial forces of 10 kN and stiffness of 2–4 kN/mm, extremely low magnetic friction of the bearing, and damping behavior [6]. While forces, stiffnesses, and friction, and their dependence on the HTS temperature satisfied our expectation, intrinsic damping of a few percent was considered to be far from effective rotor damping capability. Our assumptions and observations were consistent with the reports given by other FESS developing groups.

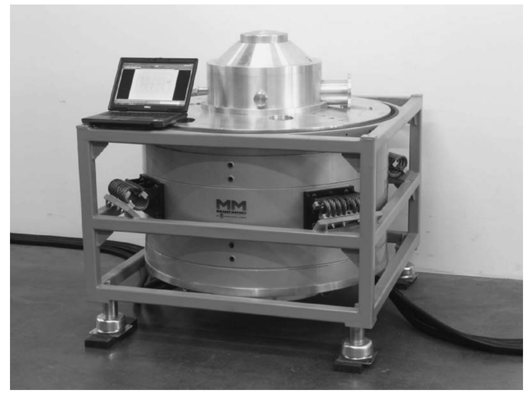

Fig. 1. ATZ/MM HTS flywheel.

Our technical concept of the HTS bearing on top and the PM bearing below the motor/generator was redesigned relative to the expected magnitude of the rotor vibration. Two dynamical damping systems are attached at both ends of the rotor shaft. The ATZ/MM HTS FESS in Fig. 1 with the abbreviation “MDS 12” (magnetohydrodynamic storage) is now assembled and will be tested for electric performance.

II. Technical Flywheel Concept

A. Overall Flywheel Structure

The assembled HTS flywheel body without the power electronics is presented in Fig. 1, and the FESS parameter are given in Table I. The HTS flywheel cylindrical housing is fixed in a

Manuscript received October 5, 2009; revised November 10, 2009 and April 6, 2010; accepted April 14, 2010. Date of publication May 18, 2010; date of current version July 30, 2010. This paper was recommended by Associate Editor M. Noe. This work was supported by the German VDI/BMBF under Contract 13N8737 and Contract 13N8738.

F. N. Werfel, U. Floegel-Delor, T. Riedel, R. Rothfeld, D. Wippich, and B. Goebel are with Adelwitz Technologiezentrum GmbH, 04886 Adelwitz, Germany (e-mail: werfel@t-online.de).

G. Reiner and N. Wehlau are with L-3 Communications Magnet-Motor GmbH, 82319 Starnberg, Germany.

Color versions of one or more of the figures in this paper are available online at http://ieeexplore.ieee.org.

Digital Object Identifier 10.1109/TASC.2010.2048708

TABLE I
HTS FLYWHEEL PARAMETERS

Parameter	value
Footprint [m^2]	1.2 x 1.2
Total height [m]	1.0
Housing diameter [m]	1.1
Total weight [t]	1.2
Rotor weight [t]	0.6
Rotor diameter [m]	~ 1
Rotor speed [rpm]	10 000 max.
Storage capacity [kWh]	10 max.
Power [kW]	250

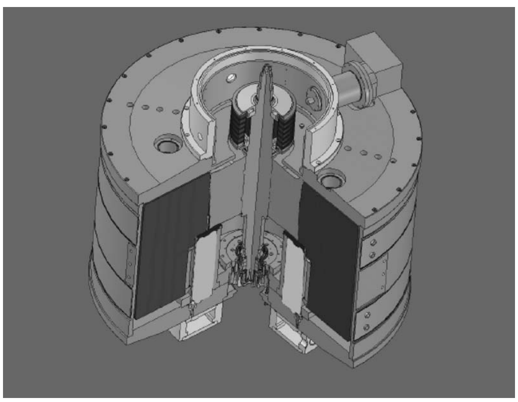

Fig. 2. HTS flywheel inner structure.

steel frame with four flexible carrying elements at the corners. Inside the container, the components with the carbon/glass fiber rotor, the concentrical motor/generator, and bearings are assembled on a central shaft. A dynamical emergency bearing and magnetic bearing are located at each end of the shaft and guarantee the precise mechanical adjustment during all rotor revolution speeds. The flywheel housing is evacuated by a rough/turbo-molecular pump combination to a basic vacuum of 10^{-2}–10^{-3} mbar. Friction experiments show the influence of air friction on the fast rotating surface of the rotor up to a pressure of about 5×10^{-3} mbar. Outgassing is expected at the beginning of the flywheel tests and will decrease with operation time.

The inner structure and architecture of the HTS FESS is given in Fig. 2. In the top position, the upper dynamical emergency bearing is located as a mechanical touchdown bearing (not shown in Fig. 2). The HTS heavy-load bearing in cylindrical symmetry is mounted in the FESS head. It provides axial and radial stiffness to the shaft and magnetically supports the total load of the rotor. A 35-W Gifford McMahon cryocooler is attached to the head of the housing. The generator/motor is controlled by a power electronic unit. Going down in Fig. 2, it follows the composite rotor with concentrically motor/generator (M/G). Below the M/G, a radial PM bearing radially stabilizes the rotor but has negative axial stiffness. This stiffness has to be compensated by the positive axial stiffness of the HTS bearing. Finally, the lower dynamical touchdown bearing with appropriate means for disengagement is assembled. It is multifunctional and supports the rotor in cases when the HTS bearing is not in operation (warm support) and in emergency situation.

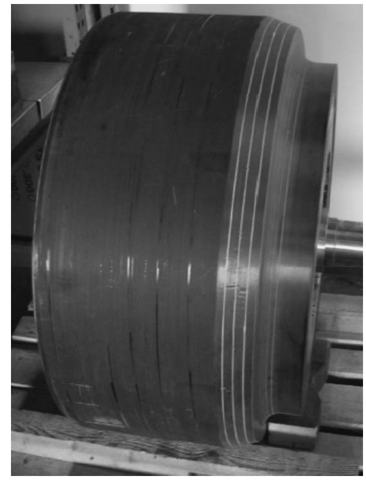

Fig. 3. Multirim flywheel rotor.

B. Glass/Carbon Fiber Rotor

The FESS has a vertical rotational axis, and all components are aligned to the central shaft (Fig. 2). The rotor in Fig. 3 is a hollow cylinder wound of glass and carbon fiber rings. It has an outer diameter of 1 m and height of 0.5 m. The rings are arranged concentrically with the stronger material toward the outer periphery where the stresses are the highest. Some of the rings are press fitted together in pairs to impose some precompression in the radial direction. The ring pairs are separated from each other by compliant elastomeric interlayer's preventing the transmission of radial stresses from one ring pair to the next. For the rotor in Fig. 3, composite rings have been press-fitted/shrink-fitted to the neighbors, again with the carbon fiber rings in the outermost layer. The multirim rotor structure shows a more even stress behavior. At a rotor speed of 10 000 r/min, the maximum rim speed is about 550 m/s, which corresponds to 40-Wh/kg specific energy. These values are 50% lower than the theoretical usable rotor parameters but are considered an industrial "fail-safe" standard. Both the kinetic energy and the hoop stress of the cylindrical rotor shell are proportional to the square of the angular velocity ω^2. In consequence of the nonlinear dependency, most of the FESS energy (75%) is stored between the maximum rotor speed and half of the top speed.

C. Motor/Generator M/G

With the M/G unit concentrically integrated in the hollow cylindrical rotor, a highly compact structure of the flywheel is obtained. The flywheel stores energy when the M/G unit works as a motor by increasing the rotor speed. Electric energy is released when the M/G is switched to the generator mode by reducing the rotor revolution per minute (r/min). The maximum storable energy capacity is determined by the rotor's mass moment of inertia and the maximum permissible rotational speed.

D. HTS Bearing

The HTS part of the top magnetic bearing, which is not shown in Fig. 2, is schematically described in Fig. 4. The

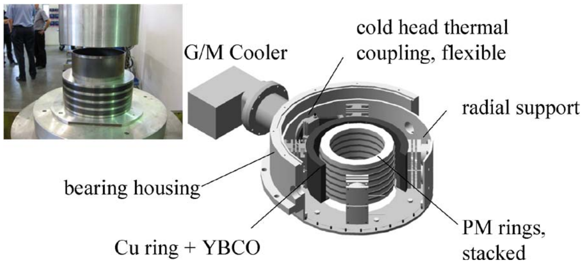

Fig. 4. Schematics of the HTS bearing structure with cold head. The insert shows part of the assembled PM rotor.

bearing itself has separately been developed, analyzed, and tested [6], [7]. The bearing is located in the head of the flywheel. The HTS part consists of multiseeded YBCO bulks machined into the segmented shape and glued into a thick wall copper ring. The copper ring is cooled by a 35-W/80-K G/M cryocooler. The bearing is mechanically supported by a G-10 structure giving high stability but having low thermal conductivity. In axial direction, the support structure was tested up to a load of 2 tons with a heat loss of less than 0.3 W.

Concentrically to the Cu/YBCO cylinder, the PM ring is connected with the flywheel shaft. The PM rings in the geometry OD 200 mm $\times$ ID 150 mm $\times$ 8 mm are stacked together with Fe flux collectors between [Fig. 4 (insert)]. The PM rings are sensitive to centrifugal forces and therefore are armed with a carbon fiber bandage. The bandage provides a prestress on the PM rings to prevent cracks or damage during high-speed operation.

E. Rotor Dynamics

Compared to mechanical bearings, the magnetic bearings are some decade's lower stiffness. Therefore, utilizing magnetic bearings for rotor stabilization, the vibration should be limited to a maximum value of 0.5 mm. First, calculations and experiments based on the stiffness values of the HTS ($k_{\mathrm{ax}} = 2$ kN/mm, $k_{\mathrm{rad}} = 1$ kN/mm) and PM bearing ($k_{\mathrm{ax}} = -1.3$ kN/mm, $k_{\mathrm{rad}} = 0.7$ kN/mm) showed that the original rotor design would cause critical rotor vibration in the millimeter range. Therefore, we decided to redesign the total rotor. In a process of calculation, measurements, and rotor rework, an optimum design with all the rotor masses was found. The amplitudes of the rotor shaft caused by possible unbalances and small tilting of the main axis of inertia could be limited to less than the critical amplitude of 0.5 mm. Due to the new construction, the rotor eigenfrequency (rigid-body critical frequency) could be shifted. In consequence, the rotor mass increased by 100 kg to more than 600 kg.

The spin whirl map diagram in Fig. 5 shows the critical speed of different modes against the rotational speed. Clearly, the low critical rpm's are caused by the magnetic bearing support. After redesigning the rotor geometry, the frequency map is calculated using a finite-element-method rotor dynamic program tool. Now, because of the magnetic bearing support, interferences occur at frequencies below 20 Hz ($\sim$1000 rpm), which is the rigid body critical frequency of the rotor. With respect to this, the flywheel speed is operating over critical.

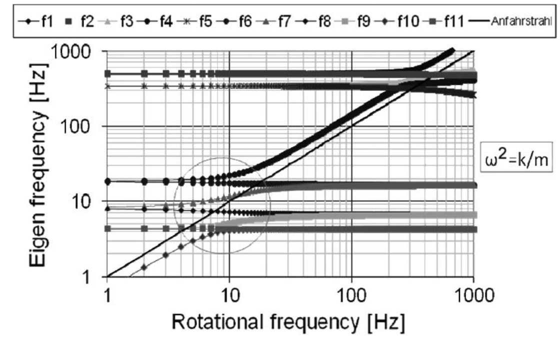

Fig. 5. Calculated diagram of flywheel rotor eigenfrequencies.

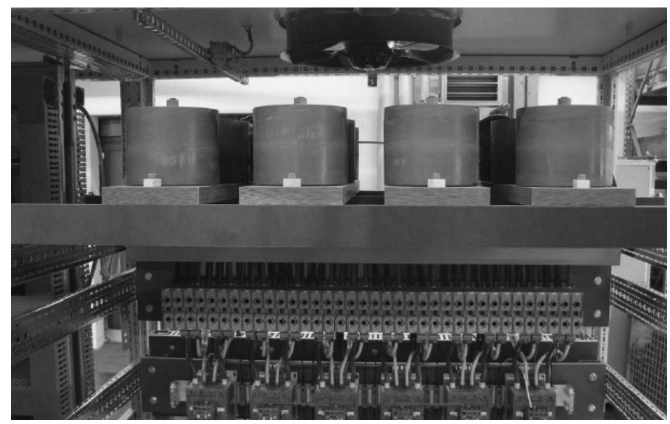

Fig. 6. Power distribution unit of the 5-kWh HTS FESS.

The low frequency amplitudes are damped by dynamical emergency bearing devices located at both ends of the rotor shaft. Possible other excitations are located above 250 Hz, which is higher than the operating range of the flywheel (0–10 000 r/min).

F. Power Electric Unit

In the industrial test, the HTS FESS will be dedicated to support a 220-V safety line in an E.ON power plant in Ingolstadt. The electric electronic part consists of a sensor system controlling various temperatures (HTS bearing, M/G, and housing), vacuum, rotor position, and vibrations. The power electric system is connected with electric feeding, control engineering, and power regulation (Fig. 6). Typically, the FESS is operating with a dc voltage in the range of 500–750 V. For safety reasons, fast power switches can separate the power electric system from the grid. The electric key element is a power management controller connected with a microprocessor interface.

In the UPS function, the FESS controls the power of a 220-V dc safety line. In case of a grid power failure, the flywheel can begin to release the energy within a few milliseconds to stabilize the grid.

III. Scaling the Flywheel Energy Storage Capacity

A. Energy Losses

Clearly, the first real HTS flywheel will not be the most efficient one. Basically, energy loss of a conventional flywheel

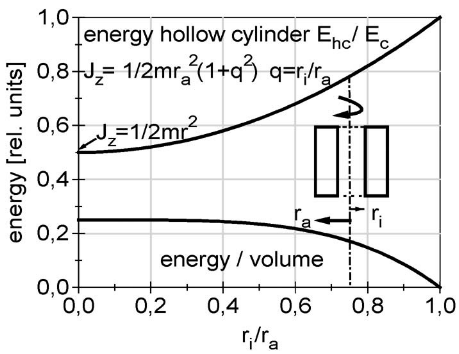

Fig. 7. Geometry and energy factors of a rotating hollow cylinder.

generally holds for 1/3 G/M, 1/3 air friction, and 1/3 mechanical bearing. It is expected that the losses of the present HTS flywheel are substantially reduced: The G/M electric losses during operation will be almost zero. The air friction is strongly reduced due to improved vacuum conditions of about 10^{-3} mbar, and the direct HTS bearing loss is a few watts. The present GM cooler rather inefficiently operates $(\mathrm{COP} \sim 2\%)$. A future machine cooler of Stirling type will improve the cold power production by a factor (theoretically 10% efficiency). In addition, HTS flywheel losses increase less than linearly with scaling up the storage capacity. This effect is caused by the necessary flywheel periphery, such as cooling, power electronics, and vacuum and safety system.

B. Scaling of Storage Capacity

To get higher storage capability, one has two basic scaling factors: the size and mass of the rotor and the speed. The present MDS rotor has a geometrical shape of a hollow cylinder, which gives two fundamental benefits. The volume-saving concentric M/G design inside the hollow rotor structure simultaneously favors the more efficient storable energy per rotor mass. Fig. 7 demonstrates the calculated achievable energy storage as a function of the inner to outer rotor diameter ratio r_i/r_a. Evidently, at the same rotor diameter and mass, a thin ring close to the outer diameter can store almost twice of the energy of a rotating bulk cylinder. The energy per weight increases with the r_i/r_a ratio, whereas the corresponding energy per volume decreases. Practically, $r_i/r_a = 0.75$ is a good compromise between the energy per weight efficiency and the absolute storable energy.

The concept of rotor stabilization provided here allows a substantially larger energy storage of 15–20 kWh. A larger HTS flywheel is already designed and dedicated to operate in an electric utility in Korea. Thereby, the simultaneous scaling of the electric power to 400 kW meets the requirements of industrial use.

IV. CONCLUSION

A 5-kWh 250-kW HTS flywheel has been tested and assembled in all components. Calculations and component tests have shown the necessity to incorporate two additional dynamical emergency bearings and a stiffer rotor design to stabilize the rotor dynamic in passing critical r/min's. With the flywheel improvements, larger energy storage at greater speeds can be achieved.

REFERENCES

[1] M. Strasik, P. E. Johnson, A. Day, J. A. Mittleider, M. D. Higgins, K. E. McCrary, C. R. McIver, D. Carlson, J. F. Gonder, J. Edwards, J. R. Schindler, and J. R. Hull, "Design, fabrication, and test of a 5-kWh/100-kW flywheel energy storage utilizing a high-temperature superconducting bearing," *IEEE Trans. Appl. Supercond.*, vol. 17, no. 2, pp. 2133–2137, Jun. 2007.

[2] N. Koshizuka, "R&D of superconducting bearing technologies for flywheel energy storage systems," *Physica C, Superconductivity*, vol. 445/44, pp. 1103–1108, Oct. 2006.

[3] T. Ichihara, K. Matsunaga, I. Hirabyashi, M. Isono, M. Hirose, K. Yoshii, K. Kurihara, O. Saito, M. Murakami, H. Takabayashi, M. Natsumeda, and N. Koshizuka, "Application of superconducting magnetic bearings to a 10 kWh-class flywheel energy storage system," *IEEE Trans. Appl. Supercond.*, vol. 15, no. 2, pp. 2245–2248, Jun. 2005.

[4] S. O. Siems, W. R. Canders, H. Walter, and J. Bock, "Superconducting magnetic bearing for a 2 MW/10 kWh class energy storage flywheel system," *Supercond. Sci. Technol.*, vol. 17, no. 5, pp. 229–233, May 2004.

[5] F. N. Werfel, U. Floegel-Delor, T. Riedel, R. Rothfeld, D. Wippich, B. Goebel, G. Reiner, and N. Wehlau, "A compact HTS 5 kWh/250 kW flywheel energy storage system," *IEEE Trans. Appl. Supercond.*, vol. 17, no. 2, pp. 2138–2141, Jun. 2007.

[6] U. Floegel-Delor, R. Rothfeld, D. Wippich, B. Goebel, T. Riedel, and F. N. Werfel, "Fabrication of HTS bearings with ton load performance," *IEEE Trans. Appl. Supercond.*, vol. 17, no. 2, pp. 2142–2145, Jun. 2007.

[7] F. N. Werfel, U. Floegel-Delor, T. Riedel, R. Rothfeld, D. Wippich, B. Goebel, G. Reiner, and N. Wehlau, "250 kW flywheel with HTS magnetic bearing for industrial use," *J. Phys. Conf. Series*, vol. 9, p. 012 206, 2008.

Frank N. Werfel, biography not available at the time of publication.

Uta Floegel-Delor, biography not available at the time of publication.

Thomas Riedel, biography not available at the time of publication.

Rolf Rothfeld, biography not available at the time of publication.

Dieter Wippich, biography not available at the time of publication.

Bernd Goebel, biography not available at the time of publication.

Gerhard Reiner, biography not available at the time of publication.

Niels Wehlau, biography not available at the time of publication.